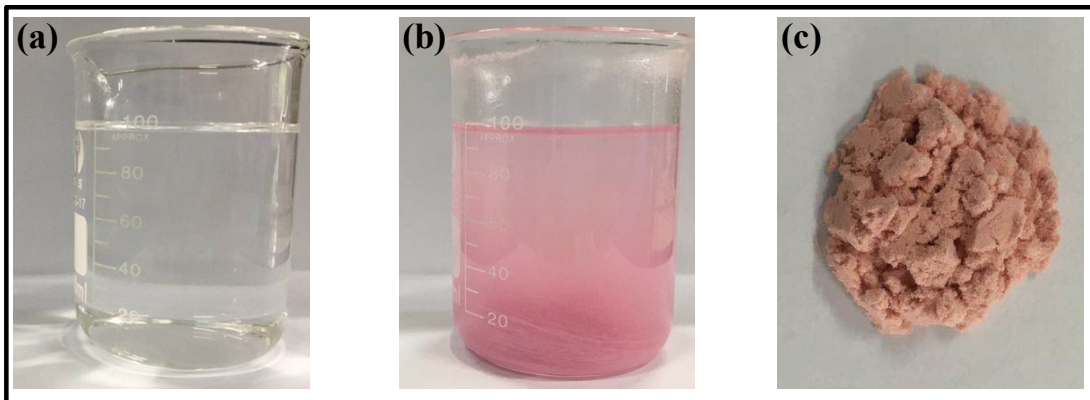


## **Tuning the activity of N-doped carbon for CO<sub>2</sub> reduction via in-situ encapsulation of nickel nanoparticles into- nano- hybrid carbon substrates**

*Cheng-Zong Yuan,<sup>†a</sup> Hong-Bao Li,<sup>†a,b\*</sup> Yi-Fan Jiang,<sup>a</sup> Kuang Liang,<sup>a</sup>  
Sheng-Jie Zhao,<sup>a</sup> Xiao-Xiang Fang,<sup>a</sup> Liu-Bo Ma,<sup>a</sup> Tan Zhao,<sup>a</sup> Cong Lin<sup>a</sup>  
and An-Wu Xu<sup>a\*</sup>*

<sup>a</sup> Division of Nanomaterials and Chemistry, Hefei National Laboratory  
for Physical Sciences at the Microscale, University of Science and  
Technology of China, Hefei 230026, China.

<sup>b</sup> Institute of Physical Science and Information Technology, Anhui  
University, Hefei 230601, China



**Fig. S1** The corresponding optical photographs of (a) Phen solution, (b) Ni-Phen in acetone solution and (c) Ni-Phen complex powder.

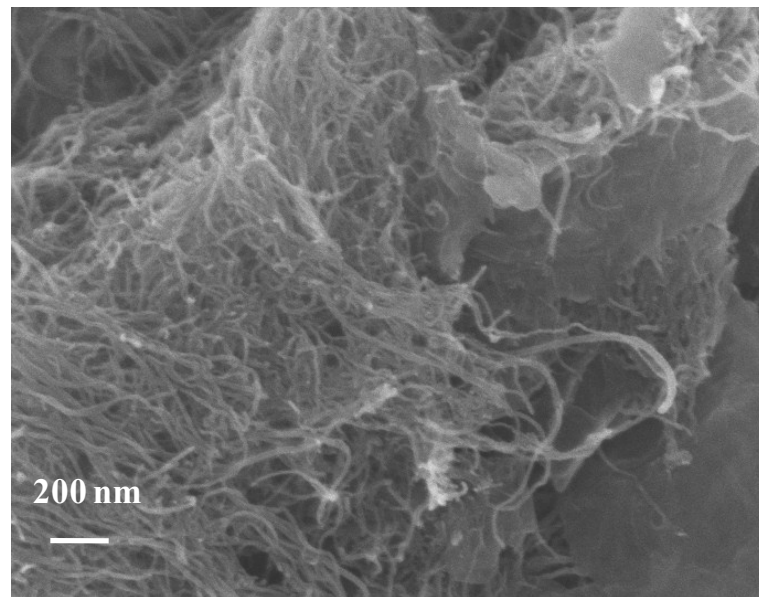


**Fig. S2** The scanning electron microscope (SEM) image of obtained N-CHS.

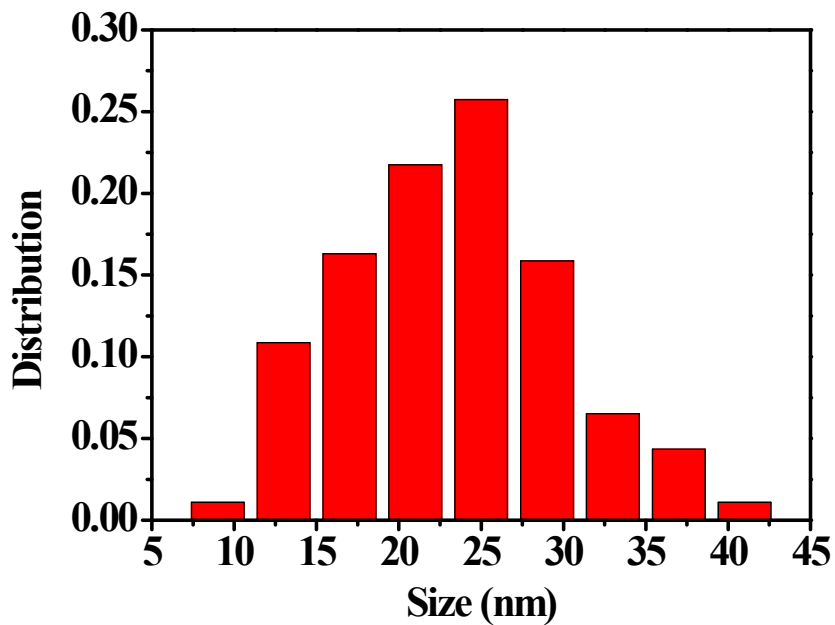


**Fig. S3** The particle size distribution of the Ni NPs on the Ni/N-CHS determined from the TEM analysis.

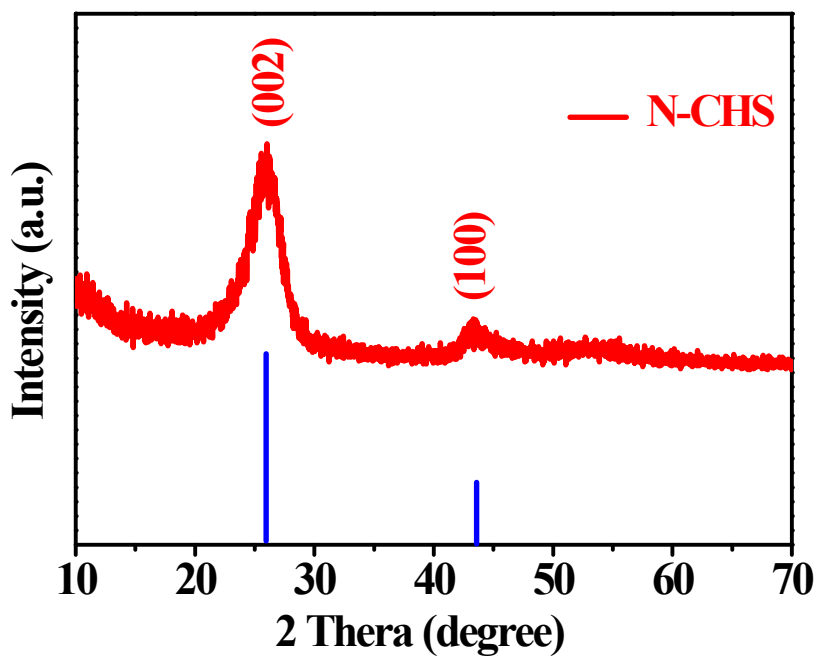


**Fig. S4** X-ray diffraction (XRD) characterization of the as-synthesized N-CHS.

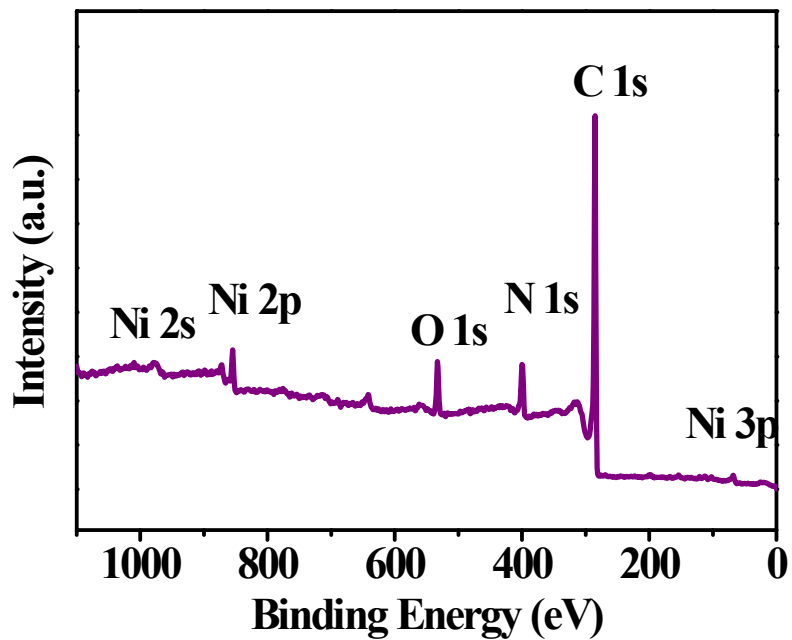


**Fig. S5** The XPS survey spectrum of Ni/N-CHS sample.

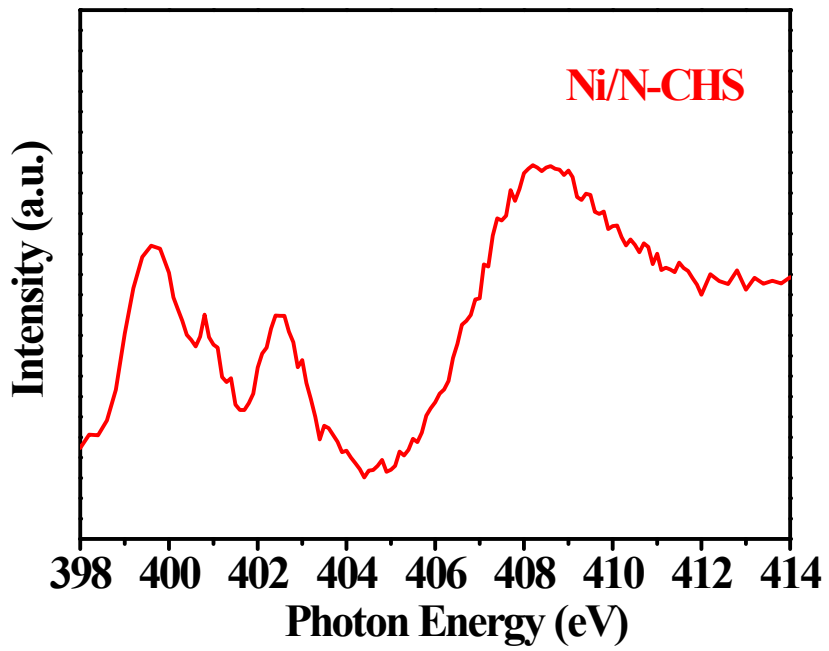


**Fig. S6** The N K-edge X-ray absorption near-edge structure (XANES) spectrum of Ni/N-CHS.

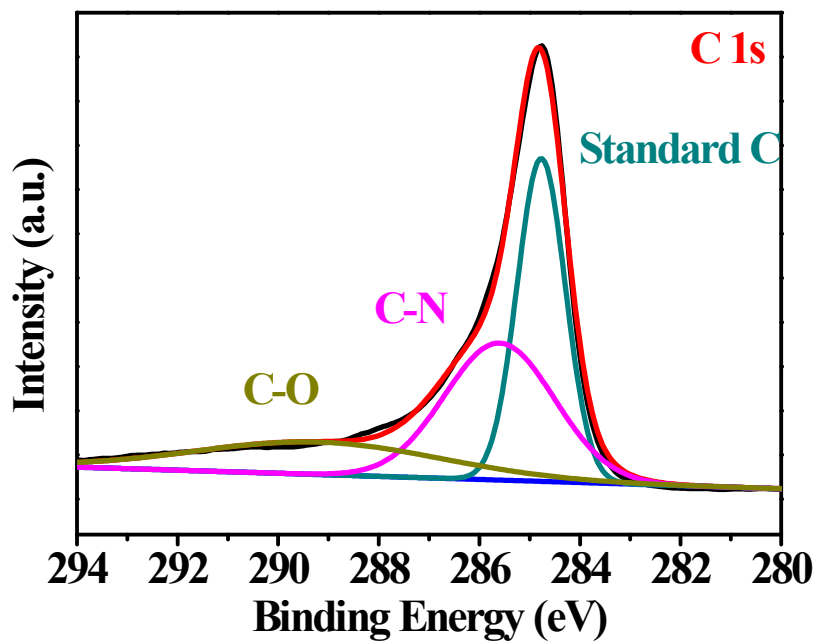


**Fig. S7** The high-resolution C 1s XPS spectrum of Ni/N-CHS.

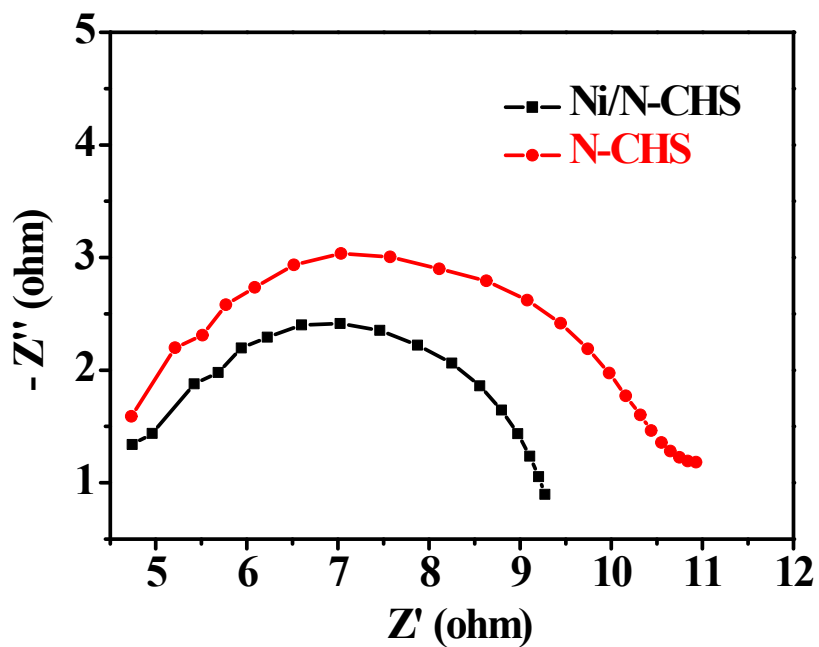


**Fig. S8** The Nyquist plots of Ni/N-CHS and N-CHS catalysts.

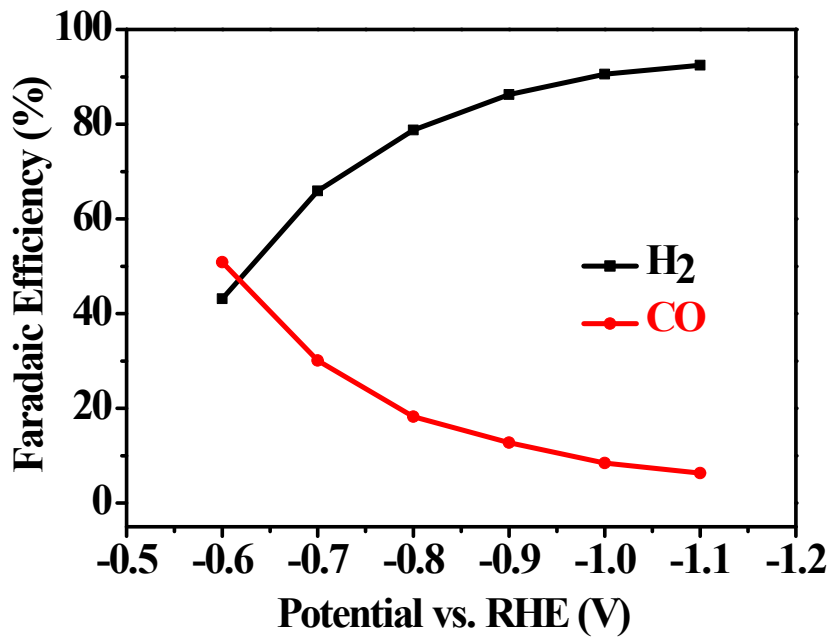


**Fig. S9** The CO<sub>2</sub>RR performances of N-C synthesized similarly without adding Ni source. The FE of CO production over N-C decreases from the potential -0.6 to -1.2 V, because the competing HER is dominant at high potential.

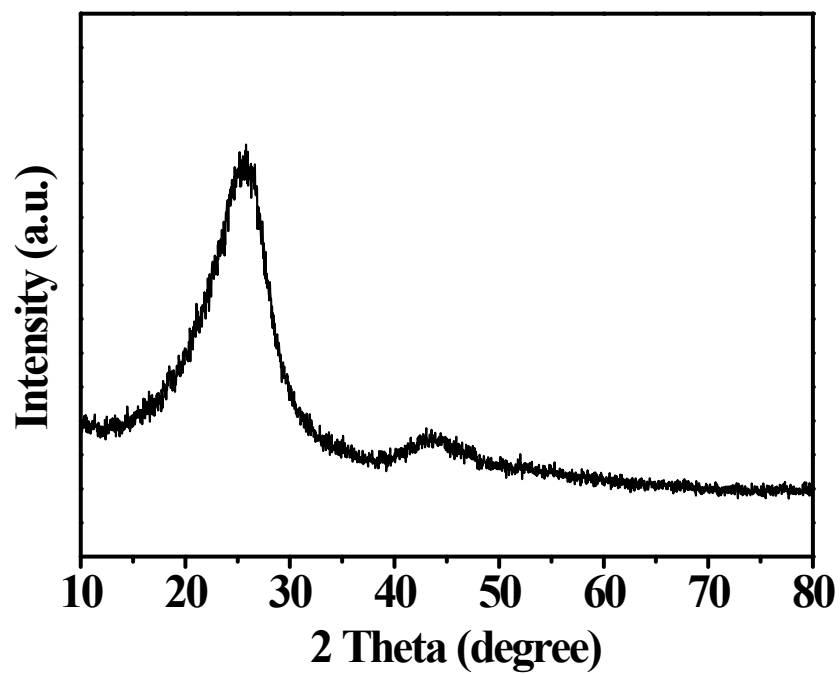


**Fig. S10** The XRD pattern of obtained N-C.

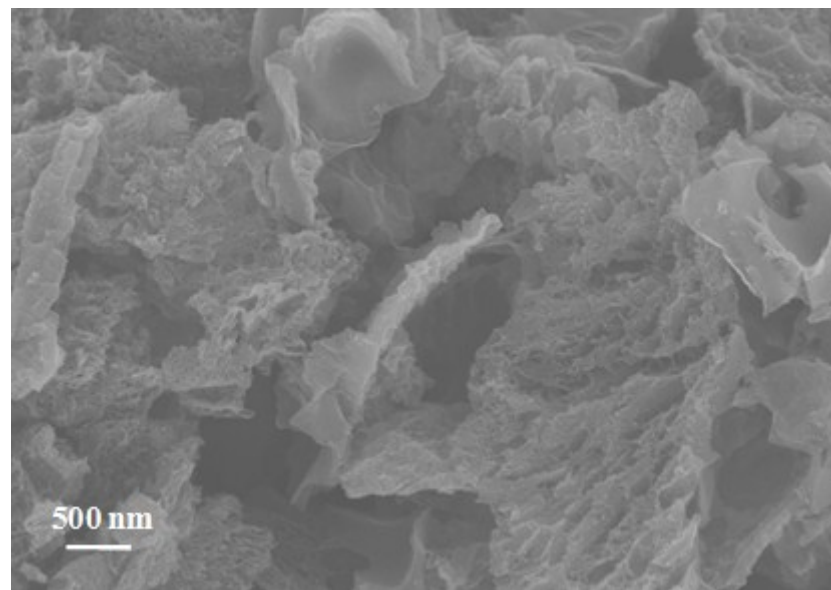


**Fig. S11** The SEM image of obtained N-C.

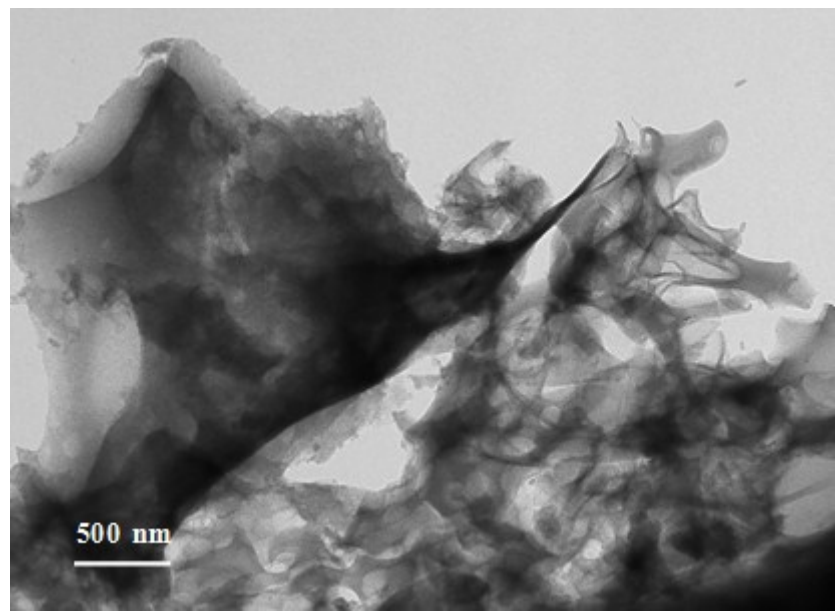


**Fig. S12** The TEM image of obtained N-C.

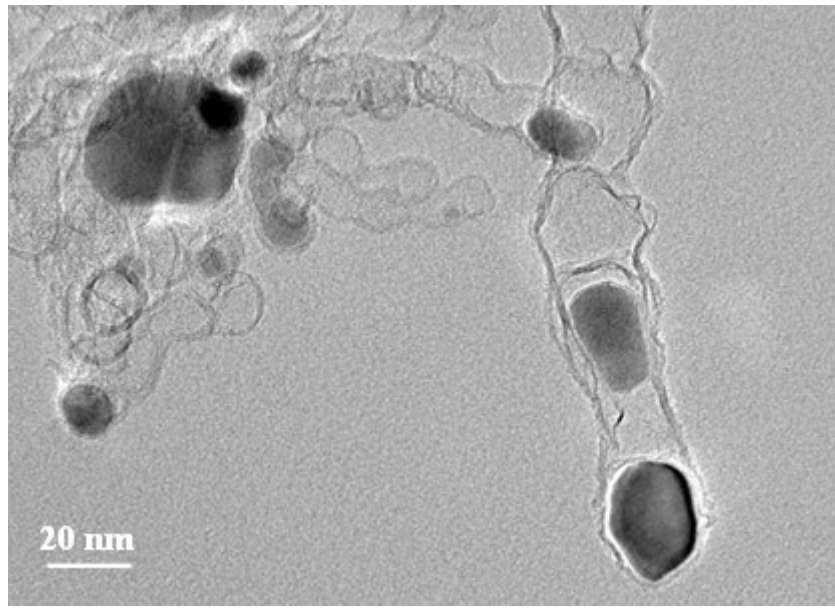


**Fig. S13** The TEM image of this catalyst after electrocatalysis.

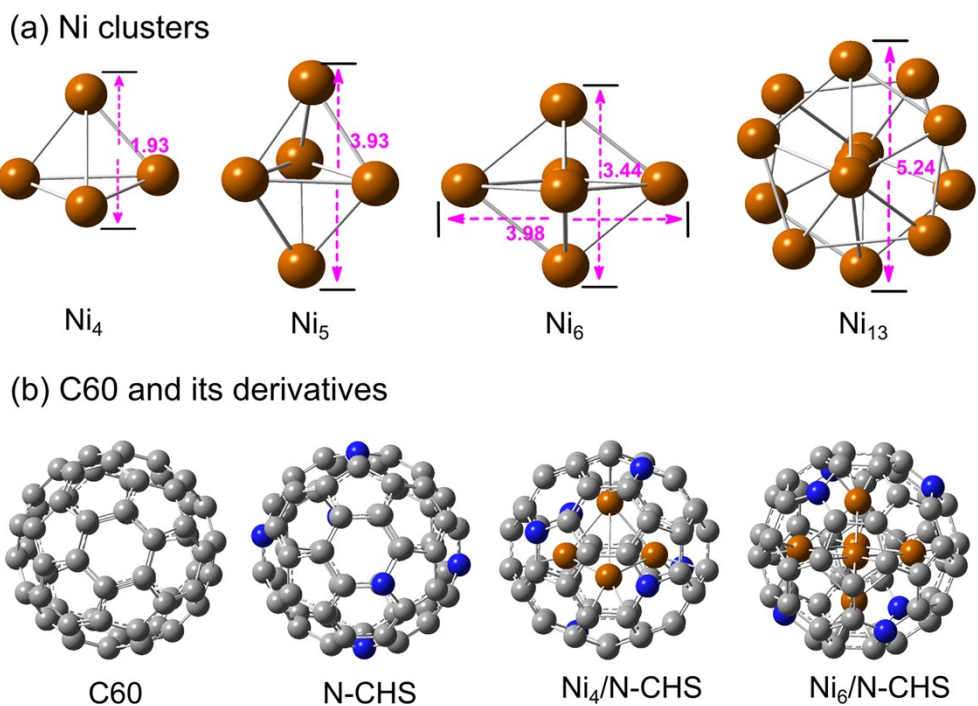


**Fig. S14** (a) Structures and sizes of the optimized Ni<sub>n</sub> clusters (n = 4, 5, 6, 10, 13). The distorted structure Ni<sub>10</sub> was abandoned. (b) C<sub>60</sub> and its various derivatives: N-CHS, Ni<sub>4</sub>/N-CHS and Ni<sub>6</sub>/N-CHS.

**Table S1.** Comparison the performances of electrochemical reduction  $\text{CO}_2$  into CO production over some state-of-the-art materials.

Catalysts	Electrolyte	Potential (V vs. RHE)	FE <sub>CO</sub> (%)	Ref.
Ni-CHS	0.5 M $\text{KHCO}_3$	- 0.9	93	This work
Pd NPs	0.1 M $\text{KHCO}_3$	- 0.89	91.2	1
Pd/C	0.5 M $\text{KHCO}_3$	- 0.6	40	2
Au NPs	0.5 M $\text{KHCO}_3$	- 0.67	90	3
Zn dendrite	0.5 M $\text{KHCO}_3$	- 1.1	79	4
Ni–N–C	0.1 M $\text{KHCO}_3$	- 0.75	85	5
Graphene foam	0.1 M $\text{KHCO}_3$	- 0.58	85	6

## References

1. D. F. Gao, H. Zhou, J. Wang, S. Miao, F. Yang, G. X. Wang, J. G. Wang and X. H. Bao, *J. Am. Chem. Soc.*, 2015, **137**, 4288–4291.
2. W. C. Sheng, S. Kattel, S. Y. Yao, B. H. Yan, Z. X. Liang, C. J. Hawxhurst, Q. Y. Wu and J. G. G. Chen, *Energy Environ. Sci.*, 2017, **10**, 1180–1185.
3. W. L. Zhu, R. Michalsky, O. Metin, H. F. Lv, S. J. Guo, C. J. Wright, X. L. Sun, A. A. Peterson and S. H. Sun, *J. Am. Chem. Soc.*, 2013, **135**, 16833–16836.
4. J. Rosen, G. S. Hutchings, Q. Lu, R. V. Forest, A. Moore and F. Jiao, *ACS Catal.*, 2015, **5**, 4586–4591.
5. W. Ju, A. Bagger, G. P. Hao, A. S. Varela, I. Sinev, V. Bon, B. R. Cuenya, S. Kaskel, J. Rossmeisl and P. Strasser, *Nat. Commun.*, 2017, **8**, 944.
6. J. J. Wu, M. J. Liu, P. P. Sharma, R. M. Yadav, L. L. Ma, Y. C. Yang, X. L. Zou, X. D. Zhou, R. Vajtai, B. I. Yakobson, J. Lou and P. M. Ajayan, *Nano Lett.*, 2016, **16**, 466–470.